doi:10.1093/brain/awl388 *Brain* (2007), **130**, 708–719

Focal atrophy in dementia with Lewy bodies on MRI: a distinct pattern from Alzheimer's disease

Jennifer L. Whitwell,[1] Stephen D. Weigand,[3] Maria M. Shiung,[1] Bradley F. Boeve,[2] Tanis J. Ferman,[5] Glenn E. Smith,[4] David S. Knopman,[2] Ronald C. Petersen,[2] Eduardo E. Benarroch,[2] Keith A. Josephs[2] and Clifford R. Jack Jr[1]

[1]Departments of Radiology, [2]Neurology (Behavioral Neurology), [3]Biostatistics, [4]Psychiatry and Psychology, Mayo Clinic, Rochester, MN and [5]Department of Psychiatry and Psychology, Mayo Clinic, Jacksonville, FL, USA

Correspondence to: Clifford R. Jack Jr, Department of Radiology, Mayo Clinic, 200 Ist St SW, Rochester, MN 55905, USA
E-mail: jack.clifford@mayo.edu

Dementia with Lewy bodies (DLB) is the second most common cause of degenerative dementia after Alzheimer's disease. However, unlike the latter, the patterns of cerebral atrophy associated with DLB have not been well established. The aim of this study was to identify a signature pattern of cerebral atrophy in DLB and to compare it with the pattern found in Alzheimer's disease. Seventy-two patients that fulfilled clinical criteria for probable DLB were age- and gender-matched to 72 patients with probable Alzheimer's disease and 72 controls. Voxel-based morphometry (VBM) was used to assess patterns of grey matter (GM) atrophy in the two patient groups, relative to controls, after correction for multiple comparisons ($P < 0.05$). Study-specific templates and prior probability maps were used to avoid normalization and segmentation bias. Region-of-interest (ROI) analyses were also performed comparing loss of the midbrain, substantia innominata (SI), temporoparietal cortex and hippocampus between the groups. The DLB group showed very little cortical involvement on VBM with regional GM loss observed primarily in the dorsal midbrain, SI and hypothalamus. In comparison, the Alzheimer's disease group showed a widespread pattern of GM loss involving the temporoparietal association cortices and the medial temporal lobes. The SI and dorsal midbrain were involved in Alzheimer's disease; however, they were not identified as a cluster of loss discrete from uninvolved surrounding areas, as observed in the DLB group. On direct comparison between the two groups, the Alzheimer's disease group showed greater loss in the medial temporal lobe and inferior temporal regions than the DLB group. The ROI analysis showed reduced SI and midbrain GM in both patient groups, with a trend for more reduction of SI GM in Alzheimer's disease than DLB, and more reduction of midbrain in DLB than Alzheimer's disease. Significantly greater loss in the hippocampus and temporo-parietal cortex was observed in the Alzheimer's disease patients when the two patient groups were compared. A pattern of relatively focused atrophy of the midbrain, hypothalamus and SI, with a relative sparing of the hippocampus and temporoparietal cortex is, therefore, suggestive of DLB and this may aid in the differentiation of DLB from Alzheimer's disease. These findings support recent pathological studies showing an ascending pattern of Lewy body progression from brainstem to basal areas of the brain. Damage to this network of structures in DLB may affect a number of different neurotransmitter systems which in turn may contribute to a number of the core clinical features of DLB.

Keywords: dementia with Lewy bodies; Alzheimer's disease; voxel-based morphometry; magnetic resonance imaging; neurotransmitter systems

Abbreviations: DLB = dementia with Lewy bodies; AD = Alzheimer's disease; GM = grey matter; ROI = region of interest; SI = substantia innominata; VBM = voxel-based morphometry; MRI = magnetic resonance imaging; MMSE = Mini-Mental Status Examination; CDR = Clinical Dementia Rating; RBD = REM sleep behaviour disorder; TIV = total intracranial volume; NBM = nucleus basalis of Meynert

Received September 19, 2006. Revised December 7, 2006. Accepted December 18, 2006. Advance Access publication January 31, 2007

Introduction

Dementia with Lewy bodies (DLB) accounts for up to 30% of all cases of dementia (Zaccai *et al.*, 2005). In contrast to Alzheimer's disease AD, which is associated with early deficits in memory, the core clinical features of DLB include fluctuating cognitive impairment, recurrent visual hallucinations and features of parkinsonism such as bradykinesia, rigidity, resting tremor and postural instability (McKeith *et al.*, 2004). Rapid eye movement sleep behaviour disorder (RBD) has also recently been recognized as an important early feature of DLB (Boeve and Saper, 2006) and has been included in the revised diagnostic criteria for the disease (McKeith *et al.*, 2005). The structural correlates of these clinical features are, however, unclear. The differential diagnosis of DLB and Alzheimer's disease can be challenging, given clinical overlap between the disorders. Clinically defined DLB cases may also have Alzheimer's disease-type pathological changes as well as the characteristic Lewy bodies (Dickson *et al.*, 1987; Josephs *et al.*, 2004). The clinical diagnostic accuracy for DLB is especially low in cases with high Braak stages of neurofibrillary tangle distribution (Merdes *et al.*, 2003). The differential diagnosis is, however, particularly important, given that patients with DLB respond well to cholinesterase inhibitors but show sensitivity to the side-effects of neuroleptic drugs (McKeith *et al.*, 2004) and there are some reports of side-effects to memantine and NMDA-antagonists (Menendez-Gonzalez *et al.*, 2005; Ridha *et al.*, 2005; Sabbagh *et al.*, 2005).

Volumetric MRI has been extensively used to characterize the patterns of cerebral atrophy in Alzheimer's disease, demonstrating involvement of the medial temporal lobe and temporo-parietal association cortices (Jack *et al.*, 1992, 1997; Fox *et al.*, 1996, 2001). However, relatively less is known about the patterns of atrophy in DLB. Studies have consistently shown that patients with DLB have less atrophy of the medial temporal lobe than patients with Alzheimer's disease (Hashimoto *et al.*, 1998; Barber *et al.*, 1999, 2000, 2001; Burton *et al.*, 2002; Ballmaier *et al.*, 2004; Tam *et al.*, 2005), but have not explicitly identified a signature pattern specific to DLB. There are inconsistencies across studies, with some showing patterns of atrophy that overlap with Alzheimer's disease (Barber *et al.*, 2002; Burton *et al.*, 2002; Almeida *et al.*, 2003; Cousins *et al.*, 2003; Ballmaier *et al.*, 2004; Brenneis *et al.*, 2004; Bozzali *et al.*, 2005), and others showing greater atrophy in specific subcortical regions, such as the putamen (Cousins *et al.*, 2003) and basal forebrain (Brenneis *et al.*, 2004; Hanyu *et al.*, 2005, 2006). The explanation for such inconsistencies and failure to replicate findings is likely due to variability in the clinical cohorts (e.g. dementia severity, symptom presentation), variability in the definition of the core clinical features (e.g. particularly fluctuating cognition), and small sample sizes.

Methodological issues regarding volumetric assessment may also account for the mixed findings in the literature. A number of the previous studies have used region-of-interest (ROI) based analyses in which only a few selected structures are assessed. These measurements are useful but can only assess those regions selected in advance. Automated techniques which look throughout the whole brain without the need for any *a priori* decisions concerning which structures to assess are now available. One such widely used technique is voxel-based morphometry (VBM) which performs a voxel-level analysis of tissue volume between groups of subjects. This technique has been widely used in studies of Alzheimer's disease but only a few studies have applied it to DLB and have found contradictory results (Burton *et al.*, 2002, 2004; Brenneis *et al.*, 2004).

The aim of this study was to identify the characteristic pattern of atrophy in patients with DLB that may aid in its differential diagnosis from Alzheimer's disease, and may shed light on the structural correlates of its core clinical features. VBM was used to assess the patterns of grey matter (GM) atrophy in a large group of prospectively studied patients clinically diagnosed with DLB relative to normal elderly controls, and to compare these patterns to those found in a large group of patients with Alzheimer's disease. In addition, ROI analyses were performed in order to validate the findings of the VBM analysis and to investigate the severity of regional differences between DLB and Alzheimer's disease.

Material and methods

Subjects and diagnosis

All subjects that fulfilled recently revised clinical criteria for probable DLB (McKeith *et al.*, 2005) and had a volumetric MRI within 4 months of the diagnosis were identified from the Mayo Clinic Alzheimer's Disease Research Center (ADRC) and Alzheimer's Disease Patient Registry (ADPR) data sets.

Clinical evaluations were carried out prospectively and the participants underwent detailed physical, neurological and neurocognitive examinations. The clinical diagnosis was based solely on clinical features without reference to imaging results. The diagnosis of DLB required the presence of at least two of the following features: visual hallucinations, fluctuations in alertness or cognition, spontaneous features of parkinsonism, or RBD (McKeith *et al.*, 2005). Visual hallucinations had to be fully formed, occurring on more than one occasion and not attributable to medical factors (e.g. infection, postoperative confusion), medications or advanced dementia. Fluctuations were considered present if the patient scored 3 or 4 on the Mayo Fluctuations Questionnaire (Ferman *et al.*, 2004). This requires 'yes' responses from caregivers to structured questions about the presence of daytime drowsiness and lethargy, sleeping during the day, staring into space for long periods of time and episodes of disorganized thought. The presence of parkinsonism required at least two of the four cardinal extrapyramidal

signs based on neurological examination (i.e. bradykinesia, rigidity, tremor and postural instability). Patients were considered to have probable RBD if they had a history of recurrent nocturnal dream enactment behaviour [i.e. met the International Classification of Sleep Disorders diagnostic criteria B for RBD, defined as abnormal, wild flailing movements occurring during sleep, with sleep-related injuries, potentially injurious behaviours or disruptions of sleep by history (AASM, 2005)].

Each subject with DLB was matched by age and gender to a cognitively normal control subject and a subject that fulfilled clinical criteria for probable Alzheimer's disease (McKhann *et al.*, 1984). The date/year that the scans were performed were also matched in an attempt to control for any temporal fluctuations associated with different scanner platform versions, although this possibility was minimized by quality control measures mentioned subsequently. All subjects were prospectively recruited into the Mayo Clinic ADRC, or the ADPR, and were identified from the ADRC/ADPR database. Control subjects were cognitively normal individuals that had been seen in internal medicine for routine physical examinations and asked to enrol in the ADRC and ADPR. All subjects were then evaluated by a neurologist to verify the normal diagnosis. Controls were identified as individuals who (i) were independently functioning community dwellers, (ii) did not have active neurological or psychiatric conditions, (iii) had no cognitive complaints, (iv) had a normal neurological and neurocognitive examination and (v) were not taking any psychoactive medications in doses that would affect cognition. Subjects that fulfilled clinical criteria for Alzheimer's disease were excluded if they had any evidence of parkinsonism. Cognitive ability across groups was assessed using the Mini-Mental Status Examination (MMSE) (Folstein *et al.*, 1975) and the Clinical Dementia Rating scale (CDR) (Hughes *et al.*, 1982).

Seventy-two subjects that fulfilled clinical criteria for DLB (McKeith *et al.*, 2005), 72 subjects with Alzheimer's disease and 72 healthy controls were identified. Twelve subjects with DLB and 16 subjects with Alzheimer's disease have since come to autopsy; 92% (11/12) of the clinically diagnosed DLB subjects had diffuse neocortical Lewy bodies on pathology and 81% (13/16) of the Alzheimer's disease subjects had Alzheimer's disease-type pathology.

Image analysis

Imaging parameters

T_1-weighted three-dimensional volumetric spoiled gradient echo (SPGR) sequences with 124 contiguous partitions and 1.6 mm slice thickness (22 × 16.5 cm FOV, 25° flip angle) were performed and used for analysis. An identical scan acquisition protocol was used for all scans. A T_1-weighted sagittal sequence with 5 mm contiguous sections was also acquired and used for the measurement of total intracranial volume (TIV). Different scanners were used, but all were GE Signa 1.5 T with body resonance module gradient sets and transmit–receive single channel head coils. All scanners undergo a standardized quality control calibration procedure daily, which monitors geometric fidelity over a 200 mm volume along all three cardinal axes, signal-to-noise and transmit gain, and maintains the scanner within a tight calibration range.

Voxel-based morphometry

An optimized method of VBM was applied, implemented using SPM2 (http://www.fil.ion.ucl.ac.uk/spm) (Ashburner and Friston, 2000; Senjem *et al.*, 2005). In order to reduce any potential normalization bias across the disease groups, customized templates and prior probability maps were created from all subjects in the study. To create the customized template and priors all images were registered to the MNI template using a 12 degrees of freedom (dof) affine transformation and segmented into GM, white matter (WM) and CSF using MNI priors. GM images were normalized to the MNI GM prior using a non-linear discrete cosine transformation (DCT). The normalization parameters were applied to the original whole head and the images were segmented using the MNI priors. Average images were created of whole head, GM, WM and CSF, and smoothed using 8 mm full-width at half-maximum (FWHM) smoothing kernel. All images were then registered to the customized whole brain template using a 12 dof affine transformation and segmented using the customized priors. The GM images were normalized to the custom GM prior using a non-linear DCT. The normalization parameters were then applied to the original whole head and the images were segmented once again using the customized priors. All images were modulated and smoothed with an 8 mm FWHM smoothing kernel. In addition, a reinitialization routine was implemented. This uses the parameters from the initial normalization to the MNI template (performed to generate the customized template) to initialize the normalization to the custom template (Senjem *et al.*, 2005).

GM differences between the DLB group and the control group, between the Alzheimer's disease group and controls, and between the DLB and Alzheimer's disease groups were assessed using the general linear model on a voxel basis after correction for multiple comparisons over the whole brain volume ($P < 0.05$). Age, gender and TIV were included in the model as nuisance variables. TIV was measured on each subject's MRI using the method described subsequently.

VBM-based ROI analysis

Mean GM density was also calculated within a number of selected ROIs using the modulated GM images generated from the VBM analysis. Previous studies have suggested that the basal forebrain, particularly the substantia innominata (SI), is a region that is particularly involved in DLB (Brenneis *et al.*, 2004; Hanyu *et al.*, 2005), even more so than in Alzheimer's disease (Mesulam and Geula, 1988; Brenneis *et al.*, 2004; Hanyu *et al.*, 2005; Teipel *et al.*, 2005). We, therefore, sought to assess the differences in mean GM volumes in this region in the DLB and Alzheimer's disease subjects. A ROI was drawn around the SI on the slice where the anterior commissure was fully visible on the unsmoothed customized template (Fig. 1). This location was chosen because the SI reaches its greatest mass under the anterior commissure (Mesulam and Geula, 1988; Teipel *et al.*, 2005), and the measurement protocol has been previously defined (Hanyu *et al.*, 2005). The lateral boundary was positioned 20 mm from the midline to the left or right side of the brain, the superior margin was defined by the edge of the anterior commissure, and the GM/CSF interface was used as the inferior boundary (Hanyu *et al.*, 2005). Another ROI was placed in the dorsal midbrain since this region was identified as being involved in the DLB group in the VBM analysis (see Results) and is a region that contains a number of central neurotransmitter nuclei that have been implicated in DLB (see Discussion). A sphere with a diameter of

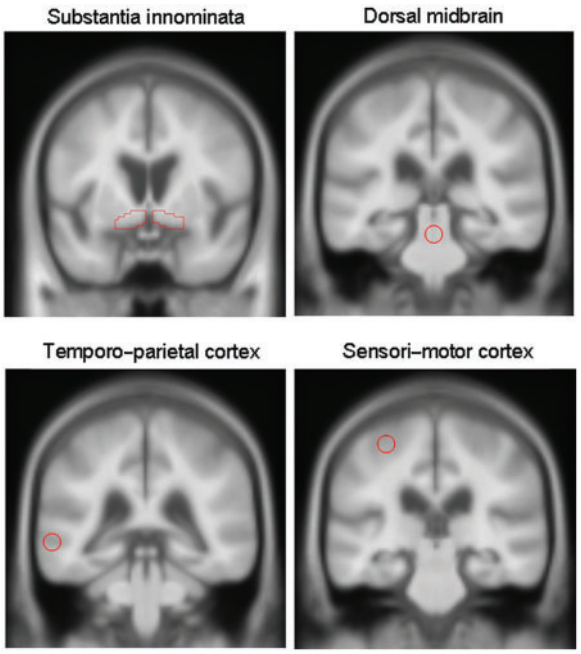

Fig. 1 Coronal slices of the unsmoothed customized template image showing the location of the four ROI used in the VBM-based ROI analysis.

5 mm was placed in the dorsal midbrain centered on the voxel showing maximum loss in the VBM analysis ($x=1$; $y=-30$; $z=-20$) (Fig. 1). Reference spherical ROIs were also then placed in the left temporoparietal cortex (diameter = 5 mm, $x=-59$, $y=-36$, $z=-2$, Fig. 1) and the left sensorimotor cortex (diameter = 5 mm, $x=-31$, $y=-27$, $z=59$, Fig. 1). We hypothesized that the Alzheimer's disease group would show greater GM loss in the temporoparietal cortex than the DLB group, whereas there would be no difference between the groups in the sensorimotor cortex.

The intensity of each voxel in the modulated GM image represents the proportion of GM present at that voxel. The median proportion of GM in each voxel was then calculated from the modulated GM images over each of the ROIs in each subject. A similar method has been applied to assess regional differences in a previous VBM study (Teipel *et al.*, 2004).

Volumetric-based ROI analysis

In addition, in order to validate the VBM-based ROI analysis a standard volumetric ROI analysis was performed. ROI were drawn around the SI, and also around the hippocampus since the VBM analysis highlighted greater involvement of the hippocampus in Alzheimer's disease than DLB. This procedure counts the number of voxels present within a region manually traced on the raw volumetric MRI scan. This contrasts with the VBM-based ROI analysis described above which estimates the proportion of GM present within a defined region on the modulated GM image. While these ROI methods use different images they both provide an estimate of volume over a defined region. All image-processing steps were performed by the same research associate who was blinded to all clinical information.

The SI measurements were performed on volumetric images that had been aligned along the anterior–posterior commissure. The contrast among the SI, globus pallidus and CSF was automatically optimized. The SI was measured on the slice where the anterior commissure was fully visible and all boundaries were defined using the protocol described in the VBM-based ROI analysis section. Hippocampal measurements were performed after several image-preprocessing steps had been performed (Jack, 1994). The borders of the left and right hippocampi were traced sequentially from posterior to anterior. In-plane hippocampal anatomic boundaries were defined to include the CA1 through CA4 sectors of the hippocampus proper, the dentate gyrus and subiculum. The posterior boundary was determined by the oblique coronal anatomic section on which the crura of the fornices were identified in full profile. The hippocampal head is defined to encompass those imaging slices extending from the intralimbic gyrus forward to the anterior termination of the hippocampal formation. Disarticulation of the hippocampal head from the amygdalae and uncinate gyrus on the anterior sections is aided by recognizing the undulating contour of the pes digitations and also by the fact that the alveus provides a high signal intensity marker defining the superior border of the head of the hippocampus formation, where it directly abuts the overlying amygalae. The inferior boundary of the hippocampus is determined by the grey–white interface formed by the subiculum and underlying parahippocampal gyrus. Test–retest reproducibility expressed as co-efficient of variation (CV) for hippocampal volume measurements has been previously measured as 0.28% (Jack *et al.*, 1998). In order to assess test–retest reproducibility for SI volume ROI measures, 21 (seven subjects from each of the three clinical groups) of the 73 cases were remeasured several weeks apart by the MRI analysis technician who was blinded to results of the original volume measurements. The CV was 0.53%. TIV was determined by tracing the margins of the inner table of the skull on contiguous images of the T1-weighted spin echo sagittal MR scan.

Statistical analysis

Due to skewness in numeric clinical measurements, we compared average values among and between groups using non-parametric methods. To confirm the effectiveness of our age matching, we compared average age across the three groups using the non-parametric Kruskal–Wallis test. Differences in years of education among the three groups were also tested with a Kruskal–Wallis test. A χ^2 test was used to assess whether the rate of APOE $\varepsilon 4$ carriers differed between DLB and Alzheimer's disease patients. MMSE and CDR sum of boxes scores were compared between DLB and Alzheimer's disease groups using two-sided Wilcoxon rank sum tests.

For group comparisons of VBM- and volumetric-based ROI data, we used linear regression models in which the ROI value was the response, group was a three-level predictor, and age, sex and TIV were included as covariates. In order to reduce skewness we log-transformed the VBM-based midbrain values, and square-root-transformed the VBM-based sensorimotor values. *P*-values for these ROIs are from the regression model and are based on a two-group contrast. For the hippocampal volume analysis we calculated age, sex and TIV adjusted *W*-scores since reference values for this ROI were available. *W*-scores can be interpreted as covariate-adjusted *Z*-scores indicating hippocampal atrophy in terms of standard deviations from normal (Jack *et al.*, 1997). For this ROI we performed two-sample *t*-tests using the *W*-scores. Since ROI differences between the DLB and control group, and the DLB and

Table 1 Patient characteristics at the time of the MRI scan

	DLB ($n=73$)	Alzheimer's disease ($n=73$)	Controls ($n=73$)	*P*-value*
No. of females (%)	17 (23.6)	17 (23.6)	17 (23.6)	–
Median (range) age, years.	73 (51–87)	76 (52–88)	74 (51–87)	0.45
Median (range) education, years	14 (8–20)	13 (8–20)	15 (8–20)	0.21
No. of APOE ε4 carriers (%)[a]	35 (50.7)	45 (67.2)	23 (32.4)	<0.001[b]
Median MMSE score (range)	22 (4–29)	21 (3–27)	29 (23–30)	0.039
Median CDR sum of boxes (range)	5 (1–15)	6 (0–15)	0 (0, 0)	0.64
No. on Cholinesterase inhibitors (%)	53 (73.6%)	50 (69.4%)	0 (0%)	0.71

[a]APOE genotype was unavailable for three DLB patients, five Alzheimer's disease patients, and one control. [b]DLB patients had a lower ε4 frequency compared with Alzheimer's disease ($P=0.076$) and higher ε4 frequency compared with controls ($P=0.042$). DLB, dementia with Lewy bodies. **P*-values for gender, age, education, APOE ε4 carrier and year of scan are based on comparing all three groups. Other *P*-values are based on comparing DLB with Alzheimer's disease groups.

Table 2 Frequency of core diagnostic features in the patients with DLB

Clinical feature	Frequency (%)
Parkinsonism	68/72 (94.4)
REM sleep behaviour disorder	55/72 (76.4)
Visual hallucinations	45/72 (62.5)
Fluctuations	33/72 (45.8)

REM, rapid eye movement.

Alzheimer's disease group were of distinct (albeit related) interest, we did not adjust the *P*-values for multiple comparisons. Raw, uncorrected data, have, however, been shown in the figures and tables to improve the ease of interpretation and comparison. The association between VBM-based ROI measurements and cognitive scores was assessed using partial correlation. Specifically, we calculated the partial correlation between the rank of the ROI measurement and the rank of the cognitive measurement, adjusting for age, sex and TIV. The effect of cholinesterase treatment was assessed by comparing the ROI volumes of subjects that were on cholinesterase inhibitors with those that were not, adjusting for age, sex and TIV using methods similar to those described before. The SI and hippocampal ROI volumes were calculated as total volumes (left plus right). All statistical analyses were performed using R version 2.2.1(RdevelopmentCoreTeam, 2005).

Results

Subjects

Seventy-two subjects who fulfilled clinical criteria for DLB (McKeith *et al.*, 2005), 72 subjects with Alzheimer's disease and 72 healthy controls were identified. The participant characteristics are shown in Table 1. By design there was no difference in age or gender distribution across all three subject groups. There was also no difference in education across the groups. The MMSE score was lower in the Alzheimer's disease group than the DLB group reflecting the relative overweighting of memory and language items compared with visuospatial and attention items on the MMSE, although there was no difference in overall functional impairment using the CDR. Table 2 shows the frequency of each of the core clinical features in the DLB cohort. Parkinsonism was the most common feature, present in 94% of the subjects. Features of RBD were present in 76% of subjects; 32/72 (44%) of these subjects underwent polysomnography (PSG) and had RBD confirmed according to the PSG criteria for the diagnosis of RBD (AASM, 2005). The least common feature was fluctuations which were only present in 46% of the subjects.

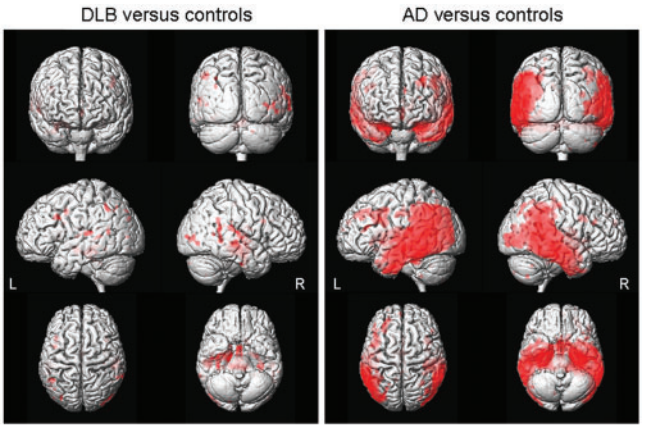

Fig. 2 Three-dimensional surface renders showing the patterns of cortical GM loss in the DLB, and Alzheimer's disease groups, compared with controls (corrected for multiple comparisons, $P<0.05$). The Alzheimer's disease group shows widespread cortical loss particularly involving the temporo-parietal cortices. In contrast, the DLB group shows very little cortical involvement.

Image analysis

Voxel-based morphometry

Very little cortical GM loss was observed in the DLB group (Fig. 2). The GM loss was instead focused on the dorsal midbrain and a region of the SI (Fig. 3). Small regions of loss were identified in the posterior hippocampus, insula and in the frontal and parietal lobes (corrected for multiple

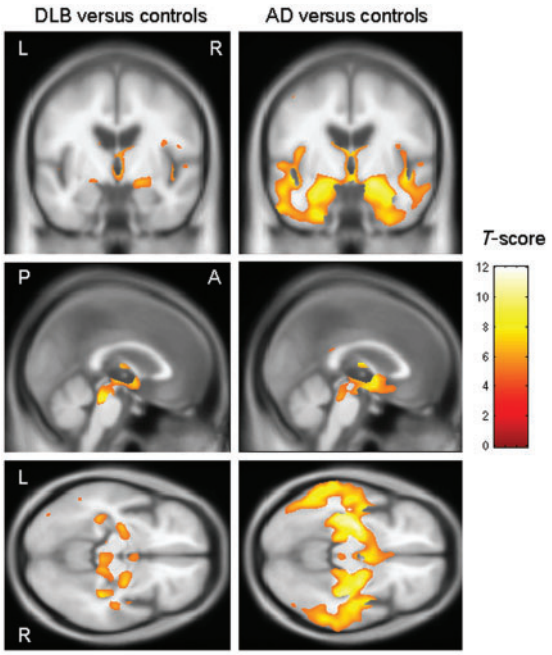

Fig. 3 Patterns of GM loss in the DLB and Alzheimer's disease groups compared with controls (corrected for multiple comparisons, $P<0.05$), overlaid on the unsmoothed customized template. This shows that the GM loss in DLB is focused on the SI, dorsal midbrain and the hypothalamus.

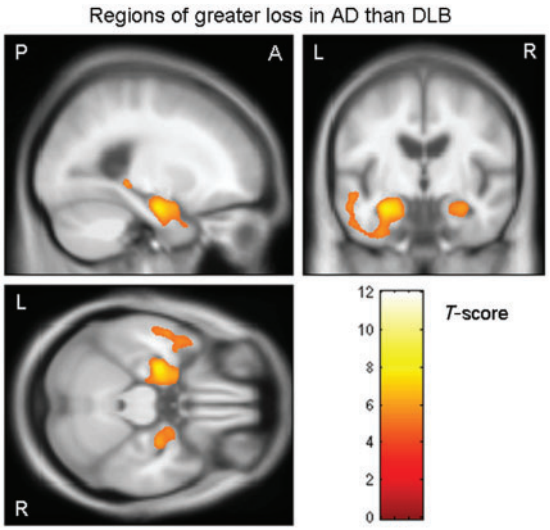

Fig. 4 Regions showing significantly greater GM loss in the Alzheimer's disease group than the DLB group (corrected for multiple comparisons, $P<0.05$), overlaid on the unsmoothed customized template.

comparisons, $P<0.05$). GM loss was also identified in a region surrounding the third ventricle.

The Alzheimer's disease group showed a widespread pattern of GM loss particularly affecting the medial temporal lobes and temporoparietal association neocortex (corrected, $P<0.05$, Fig. 2). The pattern was bilateral but showed a slight left-sided predominance. GM loss was identified throughout the temporal lobes, the posterior cingulate, insula and the inferior and middle frontal gyri. The SI and dorsal midbrain were also involved in the Alzheimer's disease group although they were not identified as discrete clusters of loss, as observed in the DLB group, but rather as part of a widespread pattern of loss (Fig. 3). Regions of GM loss were also identified around the lateral and third ventricles.

Direct comparisons between the DLB and Alzheimer's disease groups were also performed. No regions showed greater GM loss in the DLB group than the Alzheimer's disease group at the corrected threshold of $P<0.05$. However, the Alzheimer's disease group showed greater GM loss in the medial temporal lobe bilaterally, the left inferior, middle and superior temporal gyri, and in the left parietal lobe than the DLB group (corrected, $P<0.05$) (Fig. 4).

VBM-based ROI analysis

The VBM-based ROI results are shown in Table 3 and as box-plots in Fig. 5. The average GM densities in the dorsal midbrain and SI ROI were significantly lower in both the Alzheimer's disease and DLB groups compared with controls. The GM density in the dorsal midbrain was significantly lower in the DLB group than the Alzheimer's disease group ($P<0.0001$). There was no difference between the groups in the SI density, although there was a trend for lower values in the Alzheimer's disease group ($P=0.06$). The Alzheimer's disease group had significantly more GM loss in the temporoparietal cortex ROI than both the DLB and control groups ($P<0.0001$ in both), with no significant difference observed between the DLB group and controls ($P=0.25$). In addition, there were no significant differences in average GM density between any of the three groups in the sensorimotor cortex. The GM densities within each of the four ROIs did not differ between the subjects that were taking cholinesterase inhibitors and those that were not within either the Alzheimer's disease or DLB groups.

The *P*-values in Table 4 illustrate the relationships between the average GM loss in each VBM-based ROI and the cognitive scores. The MMSE and CDR scores correlated with the VBM-based ROI GM loss of the SI in the Alzheimer's disease subjects, and there was a trend for a correlation between CDR and the SI measurements in the DLB subjects. The temporoparietal cortex GM densities correlated to both the MMSE and CDR in the DLB subjects, but only to the MMSE in the Alzheimer's disease subjects. The midbrain GM densities correlated to both the MMSE and CDR in the DLB subjects, but not in the Alzheimer's disease subjects. The GM densities in the sensorimotor ROI did not correlate to either cognitive measure.

Table 3 Region-of-interest analysis results

	DLB	Alzheimer's disease	Controls
VBM-based ROI			
Substantia innominata	0.66 (0.60, 0.71)*	0.62 (0.54, 0.69)**	0.69 (0.64, 0.75)
Dorsal midbrain	0.12 (0.09, 0.16)**	0.17 (0.12, 0.22)**	0.23 (0.18, 0.29)
Temporo-parietal cortex	0.76 (0.68, 0.83)	0.65 (0.55, 0.73)**	0.79 (0.67, 0.85)
Sensori-motor cortex	0.20 (0.12, 0.31)	0.21 (0.11, 0.36)	0.23 (0.13, 0.31)
Volumetric-based ROI			
Substantia innominata	129 (120, 138)*	123 (110, 133)**	133 (124, 143)
Hippocampus	4974 (4394, 5665)**	4165 (3503, 4967)**	5468 (5059, 5856)

VBM-based ROI results are expressed as average modulated GM density per voxel, while the volumetric-based ROI results are expressed as volume in mm^3. All results are shown as median (25th percentile, 75th percentile). *Significantly different from controls at $P < 0.05$. **Significantly different from controls at $P < 0.001$.

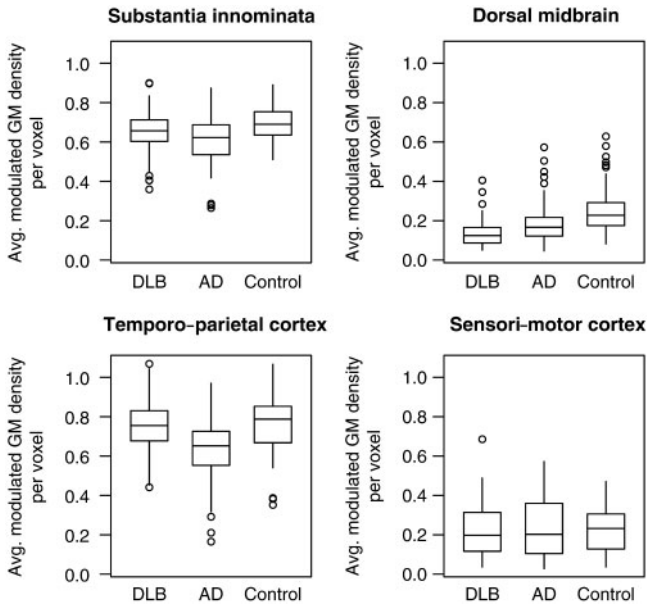

Fig. 5 Box-plots of each patient's average VBM-based modulated GM density per voxel for four ROI. The horizontal lines of the boxes represent the 25th, 50th (median) and 75th percentiles of the distributions. The vertical lines extending from the boxes stop at the most extreme data point within 1.5 interquartile ranges of the box. Points beyond this are individually identified. GM, grey matter.

Table 4 Pairwise Spearman rank-order correlation (*P*-value) between VBM-based ROI volumes and cognitive tests

Region of interest	DLB		Alzheimer's disease	
	MMSE	CDR	MMSE	CDR
Substantia innominata	0.08 (0.55)	−0.22 (0.071)	0.42 (0.001)	−0.30 (0.019)
Dorsal midbrain	0.44 (<0.001)	−0.38 (0.002)	0.25 (0.063)	−0.20 (0.13)
Temporo-parietal cortex	0.33 (0.008)	−0.34 (0.004)	0.35 (0.008)	−0.23 (0.072)
Sensori-motor cortex	0.02 (0.88)	0.01 (0.95)	0.25 (0.065)	−0.20 (0.13)

MMSE, Mini-Mental Status Examination; CDR, clinical dementia rating.

Volumetric-based ROI analysis

The volumetric-based ROI results are shown in Table 3 and as box-plots in Fig. 6. Both the DLB and Alzheimer's disease groups showed significantly smaller volumes of the SI and hippocampus than the control subjects (both $P < 0.05$). The Alzheimer's disease group showed significantly smaller volumes of the hippocampus than the DLB group ($P < 0.0001$) and a trend for smaller volumes of the SI ($P = 0.06$). The relative degree of reduction of the hippocampus and SI in Alzheimer's disease compared with DLB differed. Compared with the DLB group, the hippocampal volumes were 16% smaller in the Alzheimer's disease group, whereas the SI volumes were only 4% smaller in the Alzheimer's disease group. The volumes of the SI and hippocampus did not differ between the subjects that were taking cholinesterase inhibitors and those that were not within either the Alzheimer's disease or DLB groups.

Discussion

This study identifies a unique pattern of GM atrophy in patients with DLB that differentiates it from Alzheimer's disease. The DLB patients showed very little cortical involvement with the GM loss, which was instead focused on the dorsal midbrain, hypothalamus and the SI. While these structures were also involved in the Alzheimer's disease group they formed part of a more widespread pattern of GM loss involving the medial temporal lobes and the temporoparietal association cortices. The regions identified in the DLB patients may contribute to the relatively specific clinical features of DLB.

GM loss in the SI was identified both on the VBM analysis and in the ROI measurements. The SI contains the nucleus basalis of Meynert (NBM) which forms a major component of the cholinergic neurotransmitter system (Mesulam *et al*., 1983) (Fig. 7). Pathology is present in the NBM in DLB (Lippa *et al*., 1999; Jellinger, 2004; Tsuboi and Dickson, 2005) and previous MRI studies have demonstrated atrophy of this region in DLB (Brenneis *et al*., 2004; Hanyu *et al*., 2005). Deficits in the cholinergic system have traditionally been associated with both Alzheimer's disease and DLB, although profound cholinergic loss and severely depleted choline acetyltransferase levels occur earlier in the disease course in DLB than Alzheimer's disease (Perry *et al*., 1994; Davis *et al*., 1999; Tiraboschi *et al*., 2002). There is also some evidence that DLB patients exhibit a greater therapeutic response to cholinesterase inhibitors on average than Alzheimer's disease patients, suggesting that cholinergic deficiency is more central to symptomology in DLB (McKeith *et al*., 2000; Ellis, 2005). Atrophy of the SI was however also present in the Alzheimer's disease group. In fact, both the VBM and volumetric-based ROI analyses showed a trend towards greater involvement of the SI in Alzheimer's disease than DLB. This result is somewhat surprising given evidence that suggests earlier and more severe depletion of the cholinergic

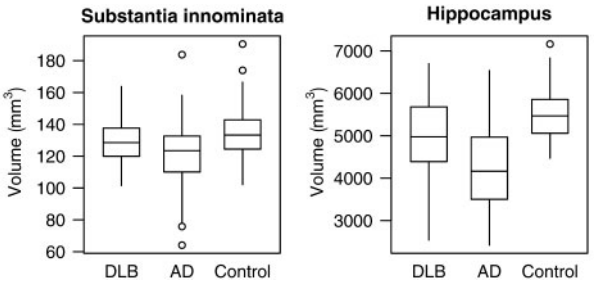

Fig. 6 Box-plots showing the hippocampal and SI volumes measured from the volumetric MRI for each subject. The horizontal lines of the boxes represent the 25th, 50th (median) and 75th percentiles of the distributions. The vertical lines extending from the boxes stop at the most extreme data point within 1.5 inter-quartile ranges of the box. Points beyond this are individually identified.

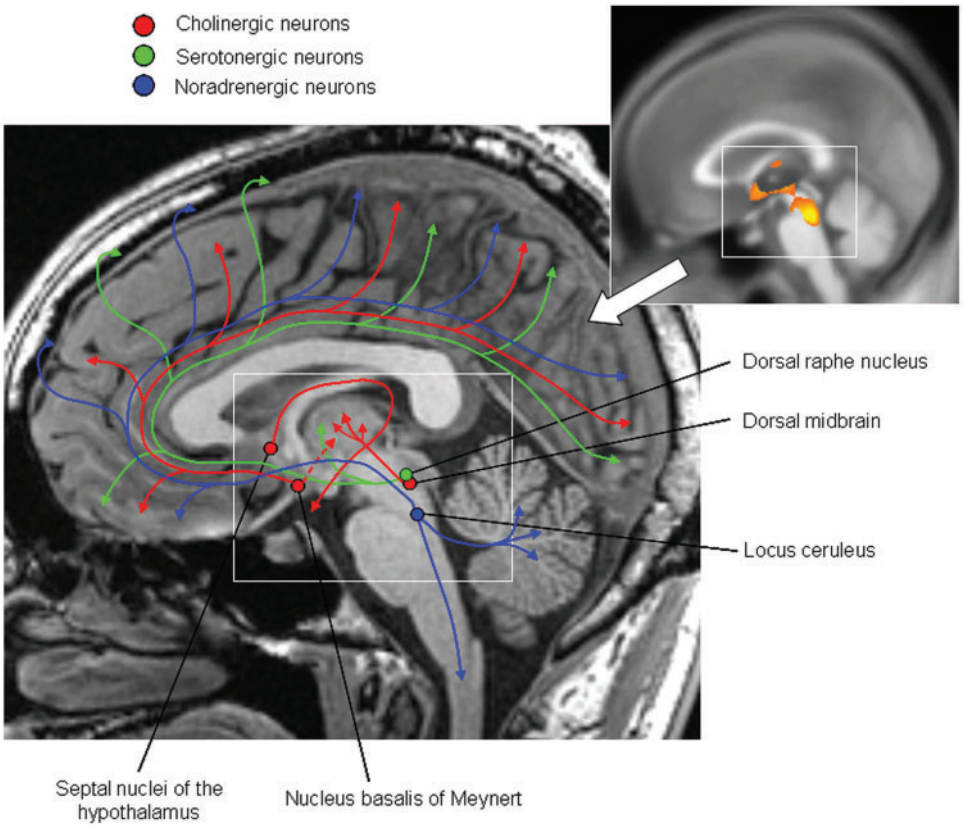

Fig. 7 Schematic diagram showing the location of cholinergic, serotonergic and noradrenergic neurons in the brainstem and basal forebrain. The inset shows the patterns of GM loss identified in the DLB group (see Fig. 3), and illustrates how the locations of the neurotransmitter nuclei correspond with the regions of loss in DLB. The cholinergic neurons in the nucleus basalis of Meynert project widely through the cingulum to the medial cerebral cortex with some lesser connections to the thalamus; neurons in the septal nuclei of the hypothalamus connect to the fornix and hippocampus (structure not shown); and neurons in the dorsal midbrain project to the thalamus. The serotonergic neurons in the dorsal raphe nucleus project to the basal ganglia and the basal forebrain, from which they distribute widely to the cerebral cortex. The noradrenergic neurons in the locus coeruleus innervate the brainstem and cerebellum, and also project to the basal forebrain, hypothalamus, temporal lobe (structure not shown) and the entire coerebral cortex (Mesulam *et al*., 1983; Mesulam and Geula, 1988; Woolsey *et al*., 2003; Benarroch, 2006).

system in DLB than Alzheimer's disease, and previous MRI studies which have shown greater involvement of the NBM in DLB than Alzheimer's disease (Brenneis *et al.*, 2004; Hanyu *et al.*, 2005). Differences across studies may reflect variability in the clinical cohorts and inclusion criteria. Alternatively, the extent of cholinergic deficits observed in DLB may occur as a result of additional damage to some of the other major cholinergic nuclei.

Two other major centres of the cholinergic system are the laterodorsal and pedunculopontine tegmental nuclei located in the dorsal midbrain (Benarroch, 2006), and the hypothalamus (Fig. 7). This study demonstrated GM volume loss in the dorsal midbrain that was greater in DLB than Alzheimer's disease. GM loss in this region correlated to worse performance on MMSE and CDR in the DLB subjects but not in the Alzheimer's disease subjects. While the midbrain has not previously been implicated in MRI studies of patients with DLB, autopsy studies have shown the midbrain to be severely involved pathologically early in the DLB disease course (Dickson *et al.*, 1987; Braak *et al.*, 2004; Jellinger, 2004). Regions of GM loss were also identified around the third ventricle in the DLB group. This most likely reflects GM loss in the surrounding regions, particularly the hypothalamus which is affected in DLB (Fujishiro *et al.*, 2006). Classification errors during segmentation commonly occur around enlarged ventricles in VBM producing an artificial rim of periventricular GM. In this case the loss was relatively focused around just the third ventricle suggesting more localized expansion. Similar findings have been interpreted as involvement of the hypothalamus in another recent study that assessed atrophy of the cholinergic nuclei in Alzheimer's disease (Teipel *et al.*, 2005). Damage to the dorsal midbrain in DLB may also affect a number of other neurotransmitter systems (Fig. 7). The noradrenergic system may be affected due to damage of the locus coeruleus which extends into the inferior midbrain region, and the serotonergic system may be affected via damage to the dorsal raphe nuclei (Benarroch, 2006). Both these nuclei are affected pathologically in DLB and Alzheimer's disease (German *et al.*, 1992; Langlais *et al.*, 1993; Szot *et al.*, 2006), although there is some evidence that they are more affected in DLB than Alzheimer's disease (Jellinger, 1990; Szot *et al.*, 2006).

The fact that the SI, midbrain and hypothalamus show greatest loss in DLB suggests that these regions are involved early in the disease course. These regions fit well with the proposed pathological progression in Parkinson's disease (PD), in which Lewy bodies have been shown to move up the brainstem into the midbrain and then to the forebrain before spreading into the cortex (Braak *et al.*, 2004). A similar pattern of progression has been suggested to occur in DLB (Jellinger, 2004). It has also been suggested that the neurons in the basal forebrain may be the most vulnerable to Lewy body pathology, and, therefore, the basal forebrain may be one of the earliest brain regions to be affected in DLB (Tsuboi and Dickson, 2005). These regions are involved much later in the Alzheimer's disease disease course (Kobayashi *et al.*, 1991; Braak and Braak, 1996).

Other scattered regions of GM loss were identified on VBM in the hippocampus, parietal lobes and frontal lobes in DLB. This fits with results from previous studies that have shown more widespread patterns of loss similar to those found in Alzheimer's disease (Burton *et al.*, 2002; Ballmaier *et al.*, 2004). Involvement of these structures could reflect underlying concurrent Alzheimer's disease pathology. The volumetric measurements of the hippocampus confirmed that hippocampal atrophy was present in the DLB group; however the degree of hippocampal atrophy was much less than that observed in the Alzheimer's disease group. The VBM analysis also showed that the medial temporal lobes were significantly more affected in the Alzheimer's disease patients than the DLB patients. These results concord with a number of previous MRI (Hashimoto *et al.*, 1998; Barber *et al.*, 1999, 2000, 2001; Burton *et al.*, 2002; Ballmaier *et al.*, 2004; Tam *et al.*, 2005) and pathological studies (Lippa *et al.*, 1998), and nicely reflect the fact that episodic/declarative memory impairment is more of a prominent early feature in Alzheimer's disease than DLB (Calderon *et al.*, 2001; Ferman *et al.*, 2006). The VBM-based ROI analysis also demonstrated significantly greater GM loss of the temporoparietal cortex in Alzheimer's disease than DLB, while as expected there was no loss in the sensorimotor cortex in either DLB or Alzheimer's disease. Loss of GM in the temporoparietal cortex correlated with the degree of clinical impairment in both the Alzheimer's disease and DLB subjects. This is somewhat surprising since the DLB group did not have significantly reduced GM density of the temporoparietal cortex compared with controls. While the majority of the DLB subjects showed very little temporoparietal loss there was overlap in the two distributions with some subjects showing loss to a similar degree to that observed in Alzheimer's disease. Again, it is likely that these may be the clinical DLB subjects that show mixed DLB and Alzheimer's disease changes on pathology. The results of the VBM and ROI analyses, therefore, suggest that assessing the patterns of atrophy of a number of different structures may provide the best discrimination of subjects with DLB and Alzheimer's disease. A pattern of SI, dorsal midbrain and hypothalamic atrophy with relative sparing of the hippocampus and temporoparietal cortex, suggests a diagnosis of DLB. While Alzheimer's disease subjects also show atrophy of the SI they show a relative sparing of the midbrain, and a characteristically more severe pattern of hippocampal and temporoparietal loss. It is important to stress, however, that this is a group study; a large degree of overlap exists between individual subjects in the Alzheimer's disease and DLB groups.

Disruption of one or more of the neurotransmitter systems may contribute to a number of the core clinical features of DLB. Deficits in the cholinergic system have

been suggested to represent the functional substrate of visual hallucinations (Perry and Perry, 1995; McKeith *et al.*, 2000; O'Brien *et al.*, 2005; Mori *et al.*, 2006), although the serotonergic system, or an imbalance between the serotonergic and cholinergic systems, could also be involved (Perry *et al.*, 1990; Cheng *et al.*, 1991; Manford and Andermann, 1998). The specific structural locus of visual hallucinations is, however, unclear. Authors have suggested that deficits in the NBM (Perry and Perry, 1995; Josephs *et al.*, 2006), or midbrain may be critical (Manford and Andermann, 1998; Josephs *et al.*, 2006). Cortical regions have also been implicated (Imamura *et al.*, 1999; Harding *et al.*, 2002; Mori *et al.*, 2006), although our study, and others, have failed to find widespread cortical atrophy in DLB (Middelkoop *et al.*, 2001). Studies have shown that fluctuations in attention may also reflect impairments of the cholinergic system, particularly in the cholinergic inputs into the thalamus (O'Brien *et al.*, 2005; Piggott *et al.*, 2006; Pimlott *et al.*, 2006). However, both the noradrenergic cells of the locus coeruleus and regions of the hypothamalus also play important roles in arousal and attention (Benarroch, 2006) and may contribute to fluctuations (Ferman *et al.*, 2004).

The neuroanatomical and neurochemical basis of the features of parkinsonism that are observed in patients with DLB are less clear. The dopaminergic system, specifically involving the substantia nigra, is predominantly affected in Parkinson's disease (Braak *et al.*, 2004), yet we observed no volume loss in the region of the substantia nigra in DLB. The probable reason that VBM does not pick up loss in the substantia nigra is due to iron deposition which results in decreased signal on the $T_2^\star$ sequence and prevents it from being detected as GM. It is, however, possible that dysfunction of the substantia nigra may result from neuronal depigmentation and gliosis without observable volume loss. Alternatively damage to other structures in the dorsal midbrain may be contributing to features of parkinsonism (Velasco *et al.*, 1979; Brooks, 1999; Kassubek *et al.*, 2002; Grafton, 2004). The neuroanatomical basis of RBD is also poorly understood but likely involves a network of structures located in the brainstem, particularly the mesopontine tegmentum and the sublaterodorsal nucleus (subcoeruleus area). These regions play crucial roles in the control of REM sleep and REM sleep atonia and it has recently been suggested that damage to the sublaterodorsal nucleus may contribute specifically to RBD (Lu *et al.*, 2006). Regions in the lower brainstem and pons segment as WM in the VBM processing and therefore would not have been picked up in our VBM analysis of GM differences.

The strength of this study is the large number of subjects in each of our subject groups and the accurate matching between groups. However, the limitations include the fact that the diagnoses were pathologically confirmed in the minority of subjects. We did, however, have autopsy data for 28 of our cases. The majority of the subjects clinically diagnosed with DLB had diffuse neocortical Lewy bodies on pathology (McKeith *et al.*, 2005). The frequency of APOE 4 in our DLB cohort is typical of previous frequencies reported in clinical cohorts (Lamb *et al.*, 1998; Singleton *et al.*, 2002), yet was higher than one might expect from pathologically confirmed cases showing only diffuse neocortical Lewy bodies suggesting that a number of our DLB subjects may have concomitant Alzheimer's disease on postmortem (Josephs *et al.*, 2004). In addition, the majority of the subjects clinically diagnosed with Alzheimer's disease had Alzheimer's disease-type pathology. The patterns of atrophy observed in this study may also reflect the clinical characteristics of our cohort. For example, the high proportion of parkinsonism may have contributed to the severe midbrain atrophy. There are also a number of limitations inherent to the techniques of normalization and segmentation within VBM, which can be a particular problem in the analysis of atrophic brains (Good *et al.*, 2002). However, these issues are not specific to this study and apply to all VBM studies on atrophic brains. The ROI measurements largely confirmed the VBM findings.

In summary, this study has shown a pattern of atrophy on MRI involving the SI, dorsal midbrain and hypothalamus in DLB. The prominent involvement of these structures differentiates it from Alzheimer's disease at a group level which showed a more widespread cortical pattern of loss. It also supports previous studies that have demonstrated greater involvement of the medial temporal lobe in Alzheimer's disease than DLB. Neurons in the SI, dorsal midbrain and hypothalamus are major components of the cholinergic system suggesting a central role of cholinergic dysfunction in DLB. However, the pattern of loss also suggests involvement of serotonergic and noradrenergic neurons. It is therefore likely that the clinical features that characterize DLB result from dysfunction of multiple neurotransmitter systems.

Acknowledgements

This study was supported by grants P50 AG16574, U01 AG06786, R01 AG11378 and R01 AG15866 from the National Institute on Aging, Bethesda MD, the generous support of the Robert H. and Clarice Smith and Abigail Van Buren Alzheimer's Disease Research Program of the Mayo Foundation, USA and by the NIH Roadmap Multidisciplinary Clinical Research Career Development Award Grant (K12/NICHD)-HD49078. D.S.K. has been a consultant to GE HealthCare, GlaxoSmithKline and Myriad Pharmaceuticals, has served on a Data Safety Monitoring Board for Neurochem Pharmaceuticals, and is an investigator in a clinical trial sponsored by Elan Pharmaceuticals. R.C.P. has been a consultant to GE Healthcare and an investigator in a clinical trial sponsored by Elan Pharmaceuticals. We would also like to acknowledge Dr Dennis Dickson and Dr Joseph Parisi for conducting the pathological analyses. Funding to pay the

Open Access Publication charges for this article was provided by Mayo Foundation.

References

AASM. International Classification of Sleep Disorders—2: Diagnostic and Coding Manual. Chicago: American Academy of Sleep Medicine; 2005.

Almeida OP, Burton EJ, McKeith I, Gholkar A, Burn D, O'Brien JT. MRI study of caudate nucleus volume in Parkinson's disease with and without dementia with Lewy bodies and Alzheimer's disease. Dement Geriatr Cogn Disord 2003; 16: 57–63.

Ashburner J, Friston KJ. Voxel-based morphometry—the methods. Neuroimage 2000; 11: 805–21.

Ballmaier M, O'Brien JT, Burton EJ, Thompson PM, Rex DE, Narr KL, et al. Comparing gray matter loss profiles between dementia with Lewy bodies and Alzheimer's disease using cortical pattern matching: diagnosis and gender effects. Neuroimage 2004; 23: 325–35.

Barber R, Ballard C, McKeith IG, Gholkar A, O'Brien JT. MRI volumetric study of dementia with Lewy bodies: a comparison with AD and vascular dementia. Neurology 2000; 54: 1304–9.

Barber R, Gholkar A, Scheltens P, Ballard C, McKeith IG, O'Brien JT. Medial temporal lobe atrophy on MRI in dementia with Lewy bodies. Neurology 1999; 52: 1153–8.

Barber R, McKeith I, Ballard C, O'Brien J. Volumetric MRI study of the caudate nucleus in patients with dementia with Lewy bodies, Alzheimer's disease, and vascular dementia. J Neurol Neurosurg Psychiatry 2002; 72: 406–7.

Barber R, McKeith IG, Ballard C, Gholkar A, O'Brien JT. A comparison of medial and lateral temporal lobe atrophy in dementia with Lewy bodies and Alzheimer's disease: magnetic resonance imaging volumetric study. Dement Geriatr Cogn Disord 2001; 12: 198–205.

Benarroch EE. Basic Neurosciences with clinical applications. Philadelphia: Elsevier; 2006.

Boeve BF, Saper CB. REM sleep behavior disorder: a possible early marker for synucleinopathies. Neurology 2006; 66: 796–7.

Bozzali M, Falini A, Cercignani M, Baglio F, Farina E, Alberoni M, et al. Brain tissue damage in dementia with Lewy bodies: an in vivo diffusion tensor MRI study. Brain 2005; 128: 1595–604.

Braak H, Braak E. Evolution of the neuropathology of Alzheimer's disease. Acta Neurol Scand Suppl 1996; 165: 3–12.

Braak H, Ghebremedhin E, Rub U, Bratzke H, Del Tredici K. Stages in the development of Parkinson's disease-related pathology. Cell Tissue Res 2004; 318: 121–34.

Brenneis C, Wenning GK, Egger KE, Schocke M, Trieb T, Seppi K, et al. Basal forebrain atrophy is a distinctive pattern in dementia with Lewy bodies. Neuroreport 2004; 15: 1711–4.

Brooks DJ. Functional imaging of Parkinson's disease: is it possible to detect brain areas for specific symptoms? J Neural Transm Suppl 1999; 56: 139–53.

Burton EJ, Karas G, Paling SM, Barber R, Williams ED, Ballard CG, et al. Patterns of cerebral atrophy in dementia with Lewy bodies using voxel-based morphometry. Neuroimage 2002; 17: 618–30.

Burton EJ, McKeith IG, Burn DJ, Williams ED, JT OB. Cerebral atrophy in Parkinson's disease with and without dementia: a comparison with Alzheimer's disease, dementia with Lewy bodies and controls. Brain 2004; 127: 791–800.

Calderon J, Perry RJ, Erzinclioglu SW, Berrios GE, Dening TR, Hodges JR. Perception, attention, and working memory are disproportionately impaired in dementia with Lewy bodies compared with Alzheimer's disease. J Neurol Neurosurg Psychiatry 2001; 70: 157–64.

Cheng AV, Ferrier IN, Morris CM, Jabeen S, Sahgal A, McKeith IG, et al. Cortical serotonin-S2 receptor binding in Lewy body dementia, Alzheimer's and Parkinson's diseases. J Neurol Sci 1991; 106: 50–5.

Cousins DA, Burton EJ, Burn D, Gholkar A, McKeith IG, O'Brien JT. Atrophy of the putamen in dementia with Lewy bodies but not Alzheimer's disease: an MRI study. Neurology 2003; 61: 1191–5.

Davis KL, Mohs RC, Marin D, Purohit DP, Perl DP, Lantz M, et al. Cholinergic markers in elderly patients with early signs of Alzheimer disease. Jama 1999; 281: 1401–6.

Dickson DW, Davies P, Mayeux R, Crystal H, Horoupian DS, Thompson A, et al. Diffuse Lewy body disease. Neuropathological and biochemical studies of six patients. Acta Neuropathol 1987; 75: 8–15.

Ellis JM. Cholinesterase inhibitors in the treatment of dementia. J Am Osteopath Assoc 2005; 105: 145–58.

Ferman TJ, Smith GE, Boeve BF, Graff-Radford NR, Lucas JA, Knopman DS, et al. Neuropscyhological differentiation of dementia with Lewy bodies from normal aging and Alzheimer's disease. Clin Neuropsychol 2006.

Ferman TJ, Smith GE, Boeve BF, Ivnik RJ, Petersen RC, Knopman D, et al. DLB fluctuations: specific features that reliably differentiate DLB from AD and normal aging. Neurology 2004; 62: 181–7.

Folstein MF, Folstein SE, McHugh PR. Mini-mental state. A practical method for grading the cognitive state of patients for the clinician. J Psychiatr Res 1975; 12: 189–98.

Fox NC, Crum WR, Scahill RI, Stevens JM, Janssen JC, Rossor MN. Imaging of onset and progression of Alzheimer's disease with voxel-compression mapping of serial magnetic resonance images. Lancet 2001; 358: 201–5.

Fox NC, Warrington EK, Freeborough PA, Hartikainen P, Kennedy AM, Stevens JM, et al. Presymptomatic hippocampal atrophy in Alzheimer's disease. A longitudinal MRI study. Brain 1996; 119: 2001–7.

Fujishiro H, Umegaki H, Isojima D, Akatsu H, Iguchi A, Kosaka K. Depletion of cholinergic neurons in the nucleus of the medial septum and the vertical limb of the diagonal band in dementia with Lewy bodies. Acta Neuropathol 2006; 111: 109–14.

German DC, Manaye KF, White CL III, Woodward DJ, McIntire DD, Smith WK, et al. Disease-specific patterns of locus coeruleus cell loss. Ann Neurol 1992; 32: 667–76.

Good CD, Scahill RI, Fox NC, Ashburner J, Friston KJ, Chan D, et al. Automatic differentiation of anatomical patterns in the human brain: validation with studies of degenerative dementias. Neuroimage 2002; 17: 29–46.

Grafton ST. Contributions of functional imaging to understanding parkinsonian symptoms. Curr Opin Neurobiol 2004; 14: 715–9.

Hanyu H, Shimizu S, Tanaka Y, Hirao K, Iwamoto T, Abe K. MR features of the substantia innominata and therapeutic implications in dementias. Neurobiol Aging 25 March 2006 [Epub ahead of print].

Hanyu H, Tanaka Y, Shimizu S, Sakurai H, Iwamoto T, Abe K. Differences in MR features of the substantia innominata between dementia with Lewy bodies and Alzheimer's disease. J Neurol 2005; 252: 482–4.

Harding AJ, Broe GA, Halliday GM. Visual hallucinations in Lewy body disease relate to Lewy bodies in the temporal lobe. Brain 2002; 125: 391–403.

Hashimoto M, Kitagaki H, Imamura T, Hirono N, Shimomura T, Kazui H, et al. Medial temporal and whole-brain atrophy in dementia with Lewy bodies: a volumetric MRI study. Neurology 1998; 51: 357–62.

Hughes CP, Berg L, Danziger WL, Coben LA, Martin RL. A new clinical scale for the staging of dementia. Br J Psychiatry 1982; 140: 566–72.

Imamura T, Ishii K, Hirono N, Hashimoto M, Tanimukai S, Kazuai H, et al. Visual hallucinations and regional cerebral metabolism in dementia with Lewy bodies (DLB). Neuroreport 1999; 10: 1903–7.

Jack CR Jr. MRI-based hippocampal volume measurements in epilepsy. Epilepsia 1994; 35 Suppl 6: S21–9.

Jack CR Jr, Petersen RC, O'Brien PC, Tangalos EG. MR-based hippocampal volumetry in the diagnosis of Alzheimer's disease. Neurology 1992; 42: 183–8.

Jack CR Jr, Petersen RC, Xu Y, O'Brien PC, Smith GE, Ivnik RJ, et al. Rate of medial temporal lobe atrophy in typical aging and Alzheimer's disease. Neurology 1998; 51: 993–9.

Jack CR Jr, Petersen RC, Xu YC, Waring SC, O'Brien PC, Tangalos EG, et al. Medial temporal atrophy on MRI in normal aging and very mild Alzheimer's disease. Neurology 1997; 49: 786–94.

Jellinger K. New developments in the pathology of Parkinson's disease. Adv Neurol 1990; 53: 1–16.
Jellinger KA. Lewy body-related alpha-synucleinopathy in the aged human brain. J Neural Transm 2004; 111: 1219–35.
Josephs KA, Tsuboi Y, Cookson N, Watt H, Dickson DW. Apolipoprotein E epsilon 4 is a determinant for Alzheimer-type pathologic features in tauopathies, synucleinopathies, and frontotemporal degeneration. Arch Neurol 2004; 61: 1579–84.
Josephs KA, Whitwell JL, Boeve BF, Knopman DS, Tang-Wai DF, Drubach DA, et al. Visual hallucinations in posterior cortical atrophy. Arch Neurol 2006; 63: 1427–32.
Kassubek J, Juengling FD, Hellwig B, Spreer J, Lucking CH. Thalamic gray matter changes in unilateral Parkinsonian resting tremor: a voxel-based morphometric analysis of 3-dimensional magnetic resonance imaging. Neurosci Lett 2002; 323: 29–32.
Kobayashi K, Miyazu K, Fukutani Y, Nakamura I, Yamaguchi N. Morphometric study on the CH4 of the nucleus basalis of Meynert in Alzheimer's disease. Mol Chem Neuropathol 1991; 15: 193–206.
Lamb H, Christie J, Singleton AB, Leake A, Perry RH, Ince PG, et al. Apolipoprotein E and alpha-1 antichymotrypsin polymorphism genotyping in Alzheimer's disease and in dementia with Lewy bodies. Distinctions between diseases. Neurology 1998; 50: 388–91.
Langlais PJ, Thal L, Hansen L, Galasko D, Alford M, Masliah E. Neurotransmitters in basal ganglia and cortex of Alzheimer's disease with and without Lewy bodies. Neurology 1993; 43: 1927–34.
Lippa CF, Johnson R, Smith TW. The medial temporal lobe in dementia with Lewy bodies: a comparative study with Alzheimer's disease. Ann Neurol 1998; 43: 102–6.
Lippa CF, Smith TW, Perry E. Dementia with Lewy bodies: choline acetyltransferase parallels nucleus basalis pathology. J Neural Transm 1999; 106: 525–35.
Lu J, Sherman D, Devor M, Saper CB. A putative flip-flop switch for control of REM sleep. Nature 2006; 441: 589–94.
Manford M, Andermann F. Complex visual hallucinations. Clinical and neurobiological insights. Brain 1998; 121: 1819–40.
McKeith I, Del Ser T, Spano P, Emre M, Wesnes K, Anand R, et al. Efficacy of rivastigmine in dementia with Lewy bodies: a randomised, double-blind, placebo-controlled international study. Lancet 2000; 356: 2031–6.
McKeith I, Mintzer J, Aarsland D, Burn D, Chiu H, Cohen-Mansfield J, et al. Dementia with Lewy bodies. Lancet Neurol 2004; 3: 19–28.
McKeith IG, Dickson DW, Lowe J, Emre M, O'Brien JT, Feldman H, et al. Diagnosis and management of dementia with Lewy bodies: third report of the DLB Consortium. Neurology 2005; 65: 1863–72.
McKhann G, Drachman D, Folstein M, Katzman R, Price D, Stadlan EM. Clinical diagnosis of Alzheimer's disease: report of the NINCDS-ADRDA Work Group under the auspices of Department of Health and Human Services Task Force on Alzheimer's Disease. Neurology 1984; 34: 939–44.
Menendez-Gonzalez M, Calatayud MT, Blazquez-Menes B. Exacerbation of Lewy bodies dementia due to memantine. J Alzheimers Dis 2005; 8: 289–91.
Merdes AR, Hansen LA, Jeste DV, Galasko D, Hofstetter CR, Ho GJ, et al. Influence of Alzheimer pathology on clinical diagnostic accuracy in dementia with Lewy bodies. Neurology 2003; 60: 1586–90.
Mesulam MM, Geula C. Nucleus basalis (Ch4) and cortical cholinergic innervation in the human brain: observations based on the distribution of acetylcholinesterase and choline acetyltransferase. J Comp Neurol 1988; 275: 216–40.
Mesulam MM, Mufson EJ, Levey AI, Wainer BH. Cholinergic innervation of cortex by the basal forebrain: cytochemistry and cortical connections of the septal area, diagonal band nuclei, nucleus basalis (substantia innominata), and hypothalamus in the rhesus monkey. J Comp Neurol 1983; 214: 170–97.
Middelkoop HA, van der Flier WM, Burton EJ, Lloyd AJ, Paling S, Barber R, et al. Dementia with Lewy bodies and AD are not associated with occipital lobe atrophy on MRI. Neurology 2001; 57: 2117–20.
Mori T, Ikeda M, Fukuhara R, Nestor PJ, Tanabe H. Correlation of visual hallucinations with occipital rCBF changes by donepezil in DLB. Neurology 2006; 66: 935–7.
O'Brien JT, Firbank MJ, Mosimann UP, Burn DJ, McKeith IG. Change in perfusion, hallucinations and fluctuations in consciousness in dementia with Lewy bodies. Psychiatry Res 2005; 139: 79–88.
Perry EK, Haroutunian V, Davis KL, Levy R, Lantos P, Eagger S, et al. Neocortical cholinergic activities differentiate Lewy body dementia from classical Alzheimer's disease. Neuroreport 1994; 5: 747–9.
Perry EK, Marshall E, Kerwin J, Smith CJ, Jabeen S, Cheng AV, et al. Evidence of a monoaminergic-cholinergic imbalance related to visual hallucinations in Lewy body dementia. J Neurochem 1990; 55: 1454–6.
Perry EK, Perry RH. Acetylcholine and hallucinations: disease-related compared to drug-induced alterations in human consciousness. Brain Cogn 1995; 28: 240–58.
Piggott MA, Ballard CG, Dickinson HO, McKeith IG, Perry RH, Perry EK. Thalamic D 2 receptors in dementia with Lewy bodies, Parkinson's disease, and Parkinson's disease dementia. Int J Neuropsychopharmacol 1 Feb 2006; [Epub ahead of print] 1–14.
Pimlott SL, Piggott M, Ballard C, McKeith I, Perry R, Kometa S, et al. Thalamic nicotinic receptors implicated in disturbed consciousness in dementia with Lewy bodies. Neurobiol Dis 2006; 21: 50–6.
RdevelopmentCoreTeam. R Development Core Team, R: A Language and Environment for Statistical Computing, 2005.
Ridha BH, Josephs KA, Rossor MN. Delusions and hallucinations in dementia with Lewy bodies: worsening with memantine. Neurology 2005; 65: 481–2.
Sabbagh MN, Hake AM, Ahmed S, Farlow MR. The use of memantine in dementia with Lewy bodies. J Alzheimers Dis 2005; 7: 285–9.
Senjem ML, Gunter JL, Shiung MM, Petersen RC, Jack CR Jr. Comparison of different methodological implementations of voxel-based morphometry in neurodegenerative disease. Neuroimage 2005; 26: 600–8.
Singleton AB, Wharton A, O'Brien KK, Walker MP, McKeith IG, Ballard CG, et al. Clinical and neuropathological correlates of apolipoprotein E genotype in dementia with Lewy bodies. Dement Geriatr Cogn Disord 2002; 14: 167–75.
Szot P, White SS, Greenup JL, Leverenz JB, Peskind ER, Raskind MA. Compensatory changes in the noradrenergic nervous system in the locus ceruleus and hippocampus of postmortem subjects with Alzheimer's disease and dementia with Lewy bodies. J Neurosci 2006; 26: 467–78.
Tam CW, Burton EJ, McKeith IG, Burn DJ, O'Brien JT. Temporal lobe atrophy on MRI in Parkinson disease with dementia: a comparison with Alzheimer disease and dementia with Lewy bodies. Neurology 2005; 64: 861–5.
Teipel SJ, Alexander GE, Schapiro MB, Moller HJ, Rapoport SI, Hampel H. Age-related cortical grey matter reductions in non-demented Down's syndrome adults determined by MRI with voxel-based morphometry. Brain 2004; 127: 811–24.
Teipel SJ, Flatz WH, Heinsen H, Bokde AL, Schoenberg SO, Stockel S, et al. Measurement of basal forebrain atrophy in Alzheimer's disease using MRI. Brain 2005; 128: 2626–44.
Tiraboschi P, Hansen LA, Alford M, Merdes A, Masliah E, Thal LJ, et al. Early and widespread cholinergic losses differentiate dementia with Lewy bodies from Alzheimer disease. Arch Gen Psychiatry 2002; 59: 946–51.
Tsuboi Y, Dickson DW. Dementia with Lewy bodies and Parkinson's disease with dementia: are they different? Parkinsonism Relat Disord 2005; 11 Suppl 1: S47–51.
Velasco F, Velasco M, Romo R, Maldonado H. Production and suppression of tremor by mesencephalic tegmental lesions in monkeys. Exp Neurol 1979; 64: 516–27.
Woolsey TA, Hanaway J, Gado MH. The brain atlas: a visual guide to the human central nervous system. Hoboken: John Wiley & Sons; 2003.
Zaccai J, McCracken C, Brayne C. A systematic review of prevalence and incidence studies of dementia with Lewy bodies. Age Ageing 2005; 34: 561–6.